Biogeosciences
Discussions

Open Access

Marine regime shifts in ocean biogeochemical models: a case study in the Gulf of Alaska

C. Beaulieu[1], H. Cole[1,a], S. Henson[2], A. Yool[2], T. R. Anderson[2], L. de Mora[3], E. T. Buitenhuis[4], M. Butenschön[3], I. J. Totterdell[5], and J. I. Allen[3]

[1]Ocean and Earth Science, University of Southampton, Southampton, UK
[2]National Oceanography Centre, Southampton, UK
[3]Plymouth Marine Laboratory, Plymouth, UK
[4]Tyndall Centre for Climate Change research, School of Environmental Sciences, University of East Anglia, Norwich, UK
[5]Hadley Centre, Met Office, Exeter, UK
[a]now at: MSS Marine Laboratory, Marine Scotland Science, Aberdeen, UK

Correspondence to: C. Beaulieu (c.beaulieu@soton.ac.uk)

Published by Copernicus Publications on behalf of the European Geosciences Union.

Discussion Paper | Discussion Paper | Discussion Paper | Discussion Paper |

BGD

12, 14003–14048, 2015

Marine regime shifts in ocean biogeochemical models

C. Beaulieu et al.

Title Page

Abstract | Introduction

Conclusions | References

Tables | Figures

◀ | ▶

◀ | ▶

Back | Close

Full Screen / Esc

Printer-friendly Version

Interactive Discussion

Abstract

Regime shifts have been reported in many marine ecosystems, and are often expressed as an abrupt change occurring in multiple physical and biological components of the system. In the Gulf of Alaska, a regime shift in the late 1970s was observed, indicated by an abrupt increase in sea surface temperature and major shifts in the catch of many fish species. This late 1970s regime shift in the Gulf of Alaska was followed by another shift in the late 1980s, not as pervasive as the 1977 shift, but which nevertheless did not return to the prior state. A thorough understanding of the extent and mechanisms leading to such regime shifts is challenged by data paucity in time and space. We investigate the ability of a suite of ocean biogeochemistry models of varying complexity to simulate regime shifts in the Gulf of Alaska by examining the presence of abrupt changes in time series of physical variables (sea surface temperature and mixed layer depth), nutrients and biological variables (chlorophyll, primary productivity and plankton biomass) using change-point analysis. Our study demonstrates that ocean biogeochemical models are capable of simulating the late 1970s shift, indicating an abrupt increase in sea surface temperature forcing followed by an abrupt decrease in nutrients and biological productivity. This predicted shift is consistent among all the models, although some of them exhibit an abrupt transition (i.e. a significant shift from one year to the next), whereas others simulate a smoother transition. Some models further suggest that the late 1980s shift was constrained by changes in mixed layer depth. Our study demonstrates that ocean biogeochemical can successfully simulate regime shifts in the Gulf of Alaska region, thereby providing better understanding of how changes in physical conditions are propagated from lower to upper trophic levels through bottom-up controls.

1 Introduction

Although there is no universal definition of a marine regime shift, they are typically described as an abrupt change in the ecosystem from one state to another, which is detectable in multiple physical and biological components of the system (Lees et al., 2006; Daskalov et al., 2007; Andersen et al., 2009; deYoung et al., 2008; Schwing, 2009). Generally, the magnitude of the regime shift is large and it occurs rapidly relative to the time spent in the different states (e.g. a shift from one year to the next that persists on decadal or longer time scales). The regime shift can be a linear response to an abrupt change in forcing itself (e.g. climate shift), a nonlinear response to a small change in forcing or driven by the internal dynamics of the system, although the exact mechanisms are often unknown (Andersen et al., 2009).

Key drivers of marine regime shifts include changes in ecosystem habitat, biotic processes such as dynamics of the foodweb and abiotic processes such as changes in the physical and chemical conditions (deYoung et al., 2008). These drivers can be natural or anthropogenic or a combined influence, which can increase the vulnerability of ecosystems (e.g. an ecosystem which has less resilience due to increasing human pressure tends to respond differently to natural disturbances) (Folke et al., 2004). Excessive fishing is an example of an anthropogenic biotic driver where a decrease in top predators (top-down control) can cause a trophic cascade, resulting in a new bottom-up controlled state (Daskalov et al., 2007). Abiotic factors such as global warming or ocean and atmosphere oscillations may initiate regime shifts through bottom-up control in the food web via phytoplankton or zooplankton (Cury and Shannon, 2004). Typically, climate shifts manifesting through changes in sea surface temperature or mixed layer depth leading to shifts in the biological components of the ecosystem through bottom-up control are considered the most easily identified (deYoung et al., 2008) and are the focus of this study.

Temporal and spatial scales of regime shifts may also affect their detectability (e.g. from a small scale coral reef regime shift occurring within a year to a North Pacific –

wide ecosystem regime shift taking a few years to transition) (deYoung et al., 2008; Drinkwater, 2006). Hence, detection of a shift in a large complex marine ecosystem such as the North Pacific or North Atlantic, in which there may be lags between the expression of the shift in the abiotic and biotic components of the system, may be
5 more noisy than detecting a regime shift in a small coral reef (deYoung et al., 2008).

A substantial part of the literature on regime shifts uses principal component analysis to compress a large number of time series representing the state of the ecosystem to a smaller number of uncorrelated ones. For example, Hare and Mantua (2000) reduced a total number of 100 time series of physical and biological variables representing the
10 state of the North Pacific to two leading modes of variability. The presence of regime shifts in the reduced set of time series may render the presence of shifts more evident to visual inspection, but this is often done without further significance testing (Andersen et al., 2009). In order to objectively identify the timing of a shift and distinguish it from a random fluctuation, change-point techniques can be used, especially methods
15 designed to detect multiple shifts in the mean of a time series (e.g. Andersen et al., 2009). For example, the shift detection methodology proposed by Rodionov (2004) consists of applying a t test successively to compare the means of two segments of a time series by considering all possible timings for a shift and repeats this until all shifts have been detected. This method has been applied widely in the marine regime
20 shift literature (e.g. Daskalov et al., 2007; DeYoung et al., 2008; Overland et al., 2008, 2010; Yatsu et al., 2008; Möllmann et al., 2009). However, it is not designed to distinguish a shift from a trend, which may lead to the detection of a series of spurious shifts in the presence of a background long-term trend (e.g. Spencer et al., 2011), which may be present in environmental time series due to climate change. Furthermore, it
25 may lead to the detection of spurious shifts in the presence of red noise, which creates patterns that may be interpreted as shifts, but which are purely random (e.g. Wunsch, 1999; Rudnick and Davis, 2003). Red noise is often present in biological time series such as chlorophyll (e.g. Beaulieu et al., 2013) and plankton (e.g. Di Lorenzo and Ohman, 2013), and manifests through a slow integrated response to random weather

Marine regime shifts in ocean biogeochemical models

C. Beaulieu et al.

forcings (Di Lorenzo and Ohman, 2013). Therefore, we opt for a methodology capable of separating a long-term trend from an abrupt change signal (e.g. from one year to the next) and distinguish these signals from red noise (Beaulieu et al., 2012). In order to further distinguish shifts that are a linear response to a shift in the forcing itself (e.g. climate shift) from shifts generated through a nonlinear response of some change in the forcing, also called thresholds or "tipping points" (Scheffer et al., 2009), the relationship between the forcing and the response can be explored using regression models (Bestelmeyer et al., 2011).

Regime shifts associated with changes in physical conditions have been previously reported in the North Atlantic (Drinkwater, 2006; Beaugrand et al., 2009; Alheit et al., 2014), North Sea (Reid et al., 2001; Beaugrand, 2004; McQuatters-Gollop et al., 2007), North Pacific (Polovina et al., 1995; Mantua et al., 1997; Hare and Mantua, 2000; Litzow and Mueter, 2014) and Gulf of Mexico (Karnauskas et al., 2015) as well as in the Benguela upwelling system (Cury and Shannon, 2004; Van der Lingen et al., 2006), among others. The late 1970s North Pacific regime shift has been comprehensively studied (Mantua et al., 1997; McGowan et al., 1998; Francis et al., 1998; Hare and Mantua, 2000; Yatsu et al., 2008). In a composite time series of 100 physical and biological variables, an abrupt and sustained change was observed during 1976–1977 (Hare and Mantua, 2000). At that time, there was a deepening of the Aleutian low pressure system which doubled the eastward wind stress and brought cooler winds over the central North Pacific, causing a drop in SST and a deepening of the mixed layer depth (MLD). This resulted in moister and warmer air settling over the California Current and the Gulf of Alaska, which caused an increase in SST in these two regions (Mantua et al., 1997). Specifically in the Gulf of Alaska, a modelling study found that the SST warming of $\sim 1\,°C$ in 1977 was accompanied by a shoaling of the MLD by 20–30 % resulting in an increase in primary production and zooplankton biomass (Polovina et al., 1995). Increases in spring zooplankton biomass were observed (Brodeur and Ware, 1992), but due to large data gaps both in space and time, analysis of interdecadal changes using these data only provide weak evidence of change (McGowan et al., 1998). In

Marine regime shifts in ocean biogeochemical models

C. Beaulieu et al.

Title Page

Abstract | Introduction

Conclusions | References

Tables | Figures

◄ | ►

◄ | ►

Back | Close

Full Screen / Esc

Printer-friendly Version

Interactive Discussion

upper trophic levels, abrupt increases in groundfish recruitment and salmon catches were observed, while some forage fish populations collapsed with consequences for piscivorous sea birds and marine mammal populations (Anderson and Piatt, 1999). Overall the yield of fish stocks in the Gulf of Alaska increased from the 1970s to the
5 1990s (McGowan et al., 1998).

Although a climate shift occurred over the entire North Pacific, the ecological response varies between regions depending on their respective dominant processes (Schwing, 2009). For example, further south in the California Current the ecological changes associated with the 1977 climate shift were different from those that occurred
10 in the Gulf of Alaska with lower salmon catches after 1977 (Mantua et al., 1997). The late 1970s regime shift in the North Pacific was followed by another shift in the late 1980s, which was not as pervasive as the 1977 shift, but was not a return to pre 1977 conditions either (Benson and Trites, 2002). Evidence for the magnitude and extent of the regime shift and the proposed mechanism is challenged by the paucity of data
15 covering adequate time and space scales in the Gulf of Alaska. Most support for the observed biological changes comes from fisheries stock assessments, which are not designed to study how climate shifts are affecting marine ecosystems (McGowan et al., 1998). If global biogeochemical models are able to accurately simulate regime shifts, they allow for examination of the links between atmospheric forcing, oceanic circula-
20 tion and production, and human food supply. Furthermore, by properly understanding the mechanisms leading to regime shifts, models may be used to predict future regime shifts and investigate the likely impact of climate change on their frequency and intensity. By using the late 1970s and 1980s regime shifts in the Gulf of Alaska as a case study we aim to assess the ability of five global ocean biogeochemical models to sim-
25 ulate these shifts. These models were part of the UK Integrated Global Biogeochemical Modelling Network (iMarNet) intercomparison which aimed to evaluate the models' ability to simulate global-scale bulk biogeochemical properties using the same ocean general circulation model and atmospheric forcing (Kwiatkowski et al., 2014). These physically identical hindcast simulations allow any model differences to be described

Marine regime shifts in ocean biogeochemical models

C. Beaulieu et al.

Title Page

Abstract	Introduction
Conclusions	References
Tables	Figures

◄ | ►|

◄ | ►

Back | Close

Full Screen / Esc

Printer-friendly Version

Interactive Discussion

only to their representation of biogeochemical processes, thereby providing insight into the mechanisms leading to marine regime shifts.

Our analysis is organised as follows. First, we investigate whether shifts are present in the Gulf of Alaska as predicted in a multiple model intercomparison hindcast experiment iMarNet (Kwiatkowski et al., 2014; imarnet.org). More specifically, we analyse model physical variables (MLD and SST) and biological and biogeochemical variables, i.e. surface dissolved inorganic nitrogen (DIN), silica (SI), iron (FE), surface chlorophyll (CHL), integrated primary production (PP), total surface phytoplankton (PHY) and zooplankton (ZOO) biomass, for regime shifts and verify whether these shifts are internally coherent. Then, we investigate the contribution of the different physical and biological variables to the observed late 1970s and late 1980s shifts in the Gulf of Alaska and the type of forcing-response relationship that led to abrupt changes.

2 Methodology

2.1 Ocean biogeochemical models

This study uses the ocean biogeochemistry model (OBGC) outputs from the iMarNet intercomparison project. The primary aim of iMarNet was to investigate the model complexity required to adequately represent marine ecosystems (Kwiatkowski et al., 2014). The participating models were HadOCC (Palmer and Totterdell, 2001), Diat-HadOCC (Halloran et al., 2010), MEDUSA-2 (Yool et al., 2011, 2013), PlankTOM10 (Le Quéré et al., 2005) and ERSEM (Baretta et al., 1995; Blackford et al., 2004). These models cover a large span of model complexity from 7 state variables (including 2 plankton functional types; PFTs) in HadOCC through to 57 state variables (including 9 PFTs) in ERSEM. The hindcast simulations (covering the period 1957 to 2007) from each of the models were used in this study.

The key focus of the iMarNet intercomparison was to evaluate the models ability to simulate global-scale bulk properties, such as carbon and nutrient cycles, as a repre-

Marine regime shifts in ocean biogeochemical models

C. Beaulieu et al.

sentation of the marine biotic activity (Kwiatkowski et al., 2014). The different OBGC models were implemented within a common physical framework to eliminate confounding errors due to the physics that would otherwise occur if different physical models were involved. iMarNET used the NEMO ocean circulation model (Madec et al., 2008) coupled with the CICE sea-ice model (Hunke and Lipscomb, 2008) on a tripolar $1°$ grid. The models were initialised from an identical physical state in 1890 using the same 3-D biogeochemical tracer fields (although not all of these tracers were used in every model). Macronutrients (nitrate, phosphorous, silicic acid) and dissolved oxygen fields were drawn from the World Ocean Atlas 2009 (Garcia et al., 2009a, b), while fields of dissolved inorganic carbon and alkalinity were drawn from the Global Ocean Data Analysis Project (GLODAP) database (Key et al., 2004). Each model used its own source for iron fields as currently there is no comprehensive global dataset available. The remaining fields such as plankton and particulate and dissolved organic matter were initialized with arbitrary small initial conditions. Below is a brief description of the structure of each OBGC model, which is also summarised in Table 1. Additional details can be found in Kwiatkowski et al. (2014).

- The Hadley Centre Ocean Carbon Cycle (HadOCC) model is a simple NPZD (Nutrient, Phytoplankton, Zooplankton, Detritus) model consisting of one phytoplankton group and one zooplankton group. There is one nutrient pool, nitrogen, to which the cycling of carbon and alkalinity is coupled. Further details can be found in Palmer and Totterdell (2001).

- Diat-HadOCC is a descendant of HadOCC with the primary difference being the presence of 2 phytoplankton groups: diatoms and mixed phytoplankton. Further differences include the addition of the nutrients silica and iron and the effect of nutrient limitation on growth is multiplicative. Further details can be found in Halloran et al. (2010).

- Model of Ecosystem Dynamics, nutrient Utilization, Sequestration and Acidification (MEDUSA) is an intermediate complexity model comprising two phytoplank-

ton and two zooplankton groups. The ecosystem is split into small (nanophytoplankton and microzooplankton) and large (diatom and mesozooplankton) components, and non-living detrital material is similarly split to reflect its sources. Nutrient pools included in this model are nitrogen, silica and iron and the effect of nutrient limitation on growth is multiplicative. Cycles of carbon, alkalinity and dissolved oxygen are also included. Further details can be found in Yool et al. (2011, 2013).

– PlankTOM10 is a relatively complex model and has 10 PFTs (diatoms, coccolithophores, *Phaeocystis*, nitrogen fixers, picophytoplankton, mixed phytoplankton, protozoa, mesozooplankton, macrozooplankton and bacteria). The nutrient cycles included in PlankTOM10 are carbon, nitrogen, oxygen, phosphorous, silica and a simplified iron cycle, the effect of nutrient limitation on growth uses the law of the minimum. All zooplankton groups eat smaller PFTs, with preference based on size. Further details can be found in Le Quéré et al. (2005) and Buitenhuis et al. (2013).

– The European Regional Seas Ecosystem Model (ERSEM) was originally used for shelf seas and consists of both pelagic and benthic ecosystems. Four phytoplankton groups (picophytoplankton/flagellates, flagellates, large phytoplankton and diatoms), three zooplankton groups (heterotrophs, microzooplankton and mesozooplankton) and heterotrophic bacteria are represented. Each zooplankton group grazes on a preferred phytoplankton group or groups based on size. The nutrient pools consist of carbon, nitrogen, phosphorous, silica and dissolved oxygen allowing for dynamic stoichiometric internal quotas. The effect of nutrient limitation on growth is given by the maximum of the individual limitation factors. More details can be found in Blackford (1997) and Blackford et al. (2004).

Marine regime shifts in ocean biogeochemical models

C. Beaulieu et al.

2.2   Simulation

The models were run for 60 years (1890 to 1949) using repeated "normal" year (i.e. without interannual variability) forcing fields from CORE2-NYF (Common Ocean-ice Reference Experiments, version 2; Large and Yeager, 2009). Then, the models were run for 58 years (1950 to 2007) using the interannual forcing fields (CORE2-IAF). The fields provided from CORE2 were downwelling irradiance (short- and long-wave), precipitation (rain and snow), air temperature, humidity and meridional and zonal winds, which are used along with bulk formulae to calculate net heat, freshwater and momentum exchange between the ocean and atmosphere (Kwiatkowski et al., 2014). For each model, where available, time series of sea surface temperature (SST), mixed layer depth (MLD, defined as a density difference from the surface of $0.1\,\mathrm{kg\,m^{-3}}$), surface dissolved inorganic nitrogen (DIN), silica (SI), iron (FE), surface chlorophyll (CHL), integrated primary production (PP), total surface phytoplankton (PHY) and zooplankton (ZOO) biomass were extracted from 1957–2007 (same period as the observational dataset used, see section below) for the Gulf of Alaska region. The time series were averaged from monthly means to annual means and then averaged spatially across the region defined by the boundaries of 55 to 65° N and 130 to 160° W (same region as the observational dataset used, see section below).

2.3   Observational dataset

To compare shifts found in model time series to observed ones, SST data were extracted from the Extended Reconstructed Sea Surface Temperature (ERSST) dataset (version 3b) for the Gulf of Alaska downloaded from https://www.ncdc.noaa.gov/ersst/. This analysis uses the International Comprehensive Ocean–Atmosphere Data Set SST data and combines ship and buoy data (Smith and Reynolds, 2003; Smith et al., 2008). The data were available as monthly means with a spatial resolution of 2° × 2° from 1957 to 2007. The ERSST dataset was averaged spatially for each year over the Gulf of Alaska (defined by the boundaries of 55 to 65° N and 130 to 160° W) to form a time

series of annual mean SST. Comparison with observed time series for other variables (i.e. MLD, DIN, SI, FE, CHL, PP, PHY, ZOO) is not possible due to lack of data over suitable space and time scales.

2.4 Statistical analyses

For the regime shift detection, we use the change-point detection method presented in Beaulieu et al. (2012), which distinguishes shifts in a time series from long-term trends and red noise. It consists of fitting a suite of regression models to a time series with (I) constant mean, (II) shift in the mean, (III) trend, (IV) shift in the intercept of the trend and (V) shift in both the intercept and trend and discriminates between them. Figure 1 illustrates the five regression models tested in this study and their equations are presented in Table 2. This methodology is based on the Schwarz Information Criterion (SIC), which is a measure of goodness of fit based on the maximum likelihood function of a given model penalised by the number of parameters estimated to ensure balance between good fit and parsimony. We use the SIC to (1) identify the timing of the shift under a model formulation containing a shift and (2) determine which regression model (among the five fitted) provides the best fit. The SIC formulations for the five models are presented in Table 2. For the models with shift (II, IV, V), the SIC is calculated for each possible timing of a shift – the timing with the lowest SIC corresponds to the year that the shift is most likely to have occurred. For example, the most likely timing for a shift for model II would be:

$$SIC_{II}(p) = \min\{SIC_{II}(k), k = 5, \ldots, n-5\} \tag{1}$$

The search for the most likely timing for a shift excludes the first and last five data points in the time series to avoid spurious detection (Beaulieu et al., 2012). The most likely timing for a shift under models IV and V can be found similarly:

$$SIC_{IV}(p) = \min\{SIC_{IV}(k), k = 5, \ldots, n-5\} \tag{2}$$
$$SIC_{V}(p) = \min\{SIC_{V}(k), k = 5, \ldots, n-5\} \tag{3}$$

Once the SIC of the five models are computed, the smallest one is selected as the most appropriate to represent the time series (Table 2). If the SIC of a model without a shift (constant mean (I) or trend (III)) is lower than the SIC of the models with a shift (shift in the mean (II), shift in the intercept (IV) or shift in the intercept and trend (V)), no abrupt change is detected in that time series. On the other hand, if a model with shift has the smallest SIC, this indicates that there could be a shift in that time series.

There is no significance level involved with the decision rule presented above and shifts tend to be too easily detected (Beaulieu et al., 2012). Therefore, a critical value can be added to the decision rule to assess the significance of the shift based on the difference in SIC between the shift model and the null model and is determined using Monte Carlo simulations. For example, if model II is selected with the smallest SIC, the null model to compare with is model I. The shift detected in model II will be significant if

$$SIC_{II}(p) - SIC_I < c_\alpha \qquad (4)$$

where c_α is the critical value at the α critical level and is determined by Monte Carlo simulation. Similarly, when models IV or V have the smallest SIC, the shift will be significant if

$$SIC_{IV}(p) - SIC_{III} < c_\alpha \qquad (5)$$

or

$$SIC_V(p) - SIC_{III} < c_\alpha \qquad (6)$$

We generate 1000 synthetic time series randomly drawn from a Normal distribution with the same length, variance and first-order autocorrelation (if present) as the data. The SIC differences between the model with a shift (e.g. model II) and the corresponding null model (e.g. model I) are calculated. This produces a null distribution for c_α against which the observed SIC difference is compared to estimate the p value. The

⏮ | ⏭

◀ | ▶

Back | Close

Full Screen / Esc

p value here is the probability of observing a SIC difference at least as extreme as that observed under the null hypothesis of no shift in the time series. We use a 5 % critical level, i.e. we reject the null hypothesis of no shift if the p value is smaller than 0.05. This analysis is based on the assumption that the residuals of the selected model are

5 normally distributed with a constant variance, which is verified using a Lilliefors test and Fisher test (5 % critical level) respectively. Violation of these assumptions could indicate the presence of additional shifts in the time series.

This method is flexible and allows for the detection of shifts that are more complex than simply a shift in the mean. Furthermore, it distinguishes potential shifts from red

10 noise, which is important given the background climate change trend and long memory of the climate system (reflected as high first-order autocorrelation). However, this method can detect at most one shift in the time series, while there could possibly be multiple shifts over a multidecadal time period. Therefore, the shift identified will be the largest to occur in a time series, which for the Gulf of Alaska is expected to be the 1977

15 regime shift, or potentially the 1989 regime shift.

We apply this methodology to time series of physical and biological variables simulated from each of the five ocean biogeochemical models, and to observed SST, averaged over the Gulf of Alaska as described in Sects. 2.1 and 2.2 respectively. As a visual support, we also calculate cumulative sums of the z scores of each time se-

20 ries. Cumulative sums are useful for monitoring time series as they exhibit a change of slope when a shift in the time series occurs (e.g. Page, 1954). In order to identify the variables contributing most to the late 1970s shift, we also apply the methodology to the first two principal components (PC) of the physical and biological variables for each model.

25 We further investigate the physical forcing – biological response relationship in models that simulate a significant shift in the late 1970s or late 1980s in the first or second principal component. Using the approach proposed by Bestelmeyer et al. (2011), we distinguish a linear or nonlinear response to forcing. We investigate the presence of changes in physical-biological relationships before and after the shift by comparing the

regression slopes. Similar slopes before and after the shift indicate a linear response to the physical forcing, while a change in the slopes rather suggests a change in the relationship and thus, a nonlinear response. More specifically, we fit simple linear regression models such as

$$y_t = a_1 + b_1 x_t + e_t \qquad t = 1, \ldots, p$$
$$y_t = a_2 + b_2 x_t + e_t \qquad t = p + 1, \ldots, n \qquad (7)$$

where y_t represents the biological response (either CHL, PP, PHY or ZOO), x_t is the physical forcing (either SST or MLD), a_1 and b_1 are the intercept and regression slope before the shift at time p, a_2 and b_2 are the intercept and regression slope after the shift and e_t are the white noise errors. To verify whether the relationships are similar before and after the shift, we test whether the slopes are equal ($b_1 = b_2$) using the Student test statistic (with $n - 4$ degrees of freedom) described by Paternoster et al. (1998):

$$t = \frac{b_1 - b_2}{s_{b_1 - b_2}} \qquad (8)$$

$$s_{b_1 - b_2} = \sqrt{s_{b_1}^2 + s_{b_2}^2} \qquad (9)$$

where b_1 and b_2 are estimated using least squares with s_{b_1} and s_{b_2} being the respective standard errors.

3 Results

Table 3 presents the results of the change point analysis on all observational and model time series. In the observed SST time series, a statistically significant shift is detected and manifests as a rapid increase in the mean of $\sim 1\,^{\circ}\text{C}$ after a decreasing trend (Fig. 2). In the model physical time series (which are identical in all 5 OBGC models), SST exhibits the same signal as the observations: a shift in the intercept and

gradient occurring in 1976, while the MLD is best represented by a linear trend. However, the model MLD time series shows strong decadal variability with large changes occurring in the mid-1970s and at the beginning of the 1990s (Fig. 2).

The fit of the most appropriate statistical models for the biological variables for each OBGC model are presented in Appendix A (Figs. A1–A5). Statistically significant shifts are found more often in the simpler OBGC models (HadOCC, Diat-HadOCC and MEDUSA) than the complex ones (Table 3). Of the statistically significant shifts identified in these models, the majority occurred in the late 1970s. In HadOCC, the late 1970s shift corresponds to a decrease in DIN, CHL and PHY, while a large increase in PP is detected in 1991. Nevertheless, PP is decreasing over the period 1957–1990 (Fig. A1). In Diat-HadOCC, all parameters exhibit a shift in the late 1970s, although it is not significant in PHY and ZOO. The significant shifts in the late 1970s manifest as a decrease in SI, FE, CHL and PP. In MEDUSA, shifts in DIN and FE (although not significant) are identified in the late 1970s. ERSEM exhibits a significant shift in CHL in the late 1970s, while PlankTOM10 does not have any significant shifts for that period.

As a visual support for the change point analysis, cumulative sums of the z scores of each time series within each model are presented in Fig. 3. A shift in a time series is revealed by a change of slope of the cumulative sums. The change of slope in SST is sharp, as one would expect given the significant shift detected. Even though our analysis does not suggest a significant shift in MLD in the late 1970s, the cumulative sums exhibit a slight change of slope, and an additional one in the late 1980s. These changes are clearly propagated to the other parameters in HadOCC, DiatHadOCC and MEDUSA with a sharp change of slope, but smoother change in ERSEM and PlankTOM10.

Figure 4 presents the two first principal components for each model. The change-point detection methodology was applied to the first two components (Table 4), which are together able to explain at least 85 % of the variance for each model (Table 5). HadOCC exhibits a shift in 1977 in the second principal component (Table 4), which is primarily driven by DIN and SST with 74 and 19 % relative contribution respectively.

This is consistent with the results of the change-point detection analysis on individual time series presented in Table 3. Shifts in HadOCC CHL and PHY were also detected in the late 1970s, but provide a small contribution to the second principal component (4 and 2 %, respectively). Note that in HadOCC the first component explains most of the variance (75 %), which is principally driven by MLD. The first principal component in Diat-HadOCC exhibits a shift in 1977 and explains 61 % of the total variance. SI and DIN are the most important variables with relative contributions of 43 and 37 % respectively. This is consistent again with the results obtained from the individual time series, which mostly exhibit a shift in the late 1970s (Table 3), but here the relative contributions of SST, CHL, PP and FE are small (< 4 %). The key role of DIN and SI in the Diat-HadOCC late 1970s shift suggests the controlling factor is nutrient limitation (i.e. bottom up control). In MEDUSA, a shift is detected in the late 1980s in the first component, which explains 70 % of the variance. SI and DIN are again the most important variables with relative contributions of 64 and 16 % respectively (Table 5), again suggesting nutrient limitation. MLD is also important with a relative contribution of 15 % (Table 5). In ERSEM, a shift is also detected in the late 1980s in the first component (52 % total variance). Again, MLD is important, with a relative contribution of 26 %. ZOO and SI also contribute by 28 and 32 % respectively (Table 5). This suggests the importance of MLD in explaining the late 1980s shift rather than SST, and a mixture of nutrient limitation and grazer control.

We further investigate the forcing-response relationship between SST and the biological variables (CHL, PP, PHY, ZOO) in HadOCC (Fig. 5) and DiatHadOCC (Fig. 6) before and after 1977, as the shift is present in the PCs in these models. The slopes of the linear relationships between SST and the biological variables are mostly similar before and after 1977 (Table 6). This is consistent with a linear response to forcing rather than a nonlinear response to changes in SST forcing. There is one possible exception for ZOO for which the difference in slopes is significant (Table 6), which suggests a potential amplified nonlinear response. As the PCs show, both MEDUSA and ERSEM simulate a shift in the late 1980s for which MLD seems to be the main forcing.

Full Screen / Esc

Printer-friendly Version

Interactive Discussion

Therefore, the forcing-response relationship between MLD and the biological variables in MEDUSA and ERSEM before and after 1988 are presented in Figs. 7 and 8 respectively. The slopes of the linear relationships between MLD and the biological variables are not significantly different before and after 1988, suggesting a linear response to changes in MLD forcing.

4 Discussion and conclusions

Using the Gulf of Alaska as a case study, our results demonstrate the usefulness of OBGC models to infer the chain of events responsible for regime shifts, especially in regions where such analysis is challenged by a lack of observations. Although there are many definitions of regime shifts in the literature, they can be generally described as an abrupt change (e.g. from one year to the next) that occurs across both physical and biological parts of the ecosystem. Therefore, to determine if a regime shift has occurred in the five OBGC models tested here the shift has to be traceable from physical parameters through to the biological parameters. With the change-point detection method used here, we found statistically significant shifts in the late 1970s in the Gulf of Alaska simulated in five OBGC models. A shift in model SST occurred in 1976 and matched a shift in observed SST. The inferred behaviour of the ecosystem is an abrupt increase in the late 1970s in SST followed by a decrease in nutrients and productivity. All OBGC models are consistent in the direction of change, but the abruptness of the change varies among them (Fig. 3). In simpler models such as HadOCC and Diat-HadOCC, significant shifts are detected through change-point analysis in most parameters, as well as in the PCs (Tables 3–4). More specifically, DIN in HadOCC and DIN and SI in Diat-HadOCC provide the largest contributions to the late 1970s shift, suggesting that the controlling factor is nutrient limitation (i.e. bottom up control) in these models (Table 5). In HadOCC and Diat-HadOCC, we find no indication of a nonlinear response of CHL, PP and PHY to changes in SST; the relationships before and after 1977 seem linear with similar slopes. However, our results suggest an amplified response of ZOO

to SST forcings after 1977; the relationship is significantly stronger after 1977 (Table 6, Figs. 7 and 8).

In the PCs, MEDUSA, ERSEM and PlankTOM10 instead produce a shift in the late 1980s (Table 4), which coincides with the 1989 regime shift that occurred in the Gulf of Alaska. The 1989 shift is significant in MEDUSA and ERSEM, but not in PlankTOM10 (Table 4). This latter regime shift seems mainly forced by MLD and nutrients (Table 5). However, in ERSEM ZOO also provides an important contribution, showing sensitivity to top-down grazer control from zooplankton (Table 5). In MEDUSA and ERSEM, the slopes of the linear relationships between MLD and CHL, PP, PHY, ZOO are not signif-icantly different before and after 1988, again suggesting a linear response to changes in MLD forcing rather than a threshold type regime shift (Table 6, Figs. 7 and 8).

Our analysis suggests that these shifts were produced as a linear response to phys-ical forcings in lower trophic levels, showing a bottom-up response due to changes in the physical environment controlled via nutrient limitation, with a potential amplified re-sponse from ZOO (only in HadOCC and Diat-HadOCC). This result is consistent with the linear tracking window hypothesis (Hsieh and Ohman, 2006), which suggests that some populations can respond linearly to changes in the physical forcings as opposed to the often implied amplified nonlinear response to small changes in forcing (or thresh-old) (e.g. Scheffer et al., 2009). However, it must be noted that our analysis is lacking top-down controls from upper trophic levels (beyond zooplankton), and may only partly explain the observed regime shifts in the Gulf of Alaska. Many drivers (and their syn-ergistic effects) may be necessary to fully explain regime shifts (Lindegren et al., 2012; Litzow et al., 2014). To our knowledge, this was the first study investigating whether OBGC models can simulate marine regime shifts. Models including upper trophic levels able to simulate regime shifts would also be beneficial to better understand the mech-anisms leading to the shift and estimate critical thresholds, but further investigation is required. At upper trophic levels, marine ecological thresholds have been studied using predator-prey models to provide evidence of abrupt nonlinear responses of predators to changes in prey abundance (e.g. Plagányi et al., 2014).

Marine regime shifts in ocean biogeochemical models

C. Beaulieu et al.

The 1977 regime shift in the Gulf of Alaska was observed in temperature and a variety of commercial fish species (McGowan et al., 1998). Here, we are inferring the behaviour of the nutrients and plankton using OBGC models. The shift detected in SST is similar between the observations and models: both show an increase of $\sim 1\,^\circ$C after 1976. The MLD is overall increasing but does not exhibit a significant shift in the late 1970s. All models simulate a decrease in nutrients and biological productivity after the SST shift in 1976. The direction of these changes does not entirely match that expected from the conceptual model of the 1977 regime shift for the Gulf of Alaska of Polovina et al. (1995), investigating the links between climate forcing and salmon production through the effects on plankton production. The observed increase in salmon catches after the 1977 shift was hypothesized to result from an increase in productivity across the Gulf of Alaska driven by the shoaling of the MLD and the alleviation of light limitation despite a reduction in nutrient concentrations (Polovina et al., 1995; Hare and Mantua, 2000). From temperature profiles, Polovina et al. (1995) observed that the MLD was 30–40 % shallower during winter/spring after 1977 resulting in an increase in primary and secondary production. In the present study, the MLD is instead increasing. Thus the decrease in nutrients after 1977 seems to be the dominant driver in the reduction in productivity and outweighs any potential advantage to phytoplankton from increased light availability. The dominance of nutrients in explaining the variability in the principal components of HadOCC and Diat-HadOCC supports this. However, it must be noted that we use time series of annual means in the present study, while the results from Polovina et al. (1995) suggest that the important changes may be associated with specific seasons. Further analysis would be required to investigate changes at the seasonal scale and is beyond the scope of this study.

All the OBGC models used in this study have the same underlying physical model, and were run with the same initial conditions and forcing fields, but their different nutrient and biological responses indicate the role of the model ecosystem complexity in simulating regime shifts. All models simulate a decrease in nutrients and biological productivity after the SST shift in 1976. In the simpler models such as HadOCC and

Marine regime shifts in ocean biogeochemical models

C. Beaulieu et al.

⏮ | ⏭

◀ | ▶

Back | Close

Full Screen / Esc

Printer-friendly Version

Interactive Discussion

Diat-HadOCC, the shift in SST leads to a significant abrupt decrease in nutrients and biological productivity, which becomes less abrupt as the model complexity increases from MEDUSA to PlankTOM10 to ERSEM. The simpler models have fewer plankton groups responding to environmental changes (both HadOCC and Diat-HadOCC have

5 one zooplankton group, and Diat-HadOCC has two phytoplankton groups), which might explain a more direct response than a model with a larger number of plankton groups with more interactions between groups. More complex models could potentially unveil shifts in the community structure (i.e. increase of a certain type of plankton and decrease of another one), as regime shifts can affect different species in opposite ways

10 (Benson and Trites, 2002). Feedbacks and interactions between groups in the models are in need of thorough exploration to determine how they affect the simulation of regime shifts seen in observations. Such analysis should be the focus of future work.

We suggest an approach to detect shifts and distinguish them from a long-term trend and red noise (Beaulieu et al., 2012). The main limitation of this methodology is the

15 ability to detect at most one shift, but extension to multiple shifts is beyond the scope of this study. We further suggest how to distinguish between a regime shift in which a linear response to a forcing shift was observed as opposed to a nonlinear response when crossing a threshold, by analysing changes in forcing-response relationship. This idea was proposed in Bestelmeyer et al. (2011), but here we introduce a test to com-

20 pare the forcing-response relationship before and after the shift. This approach can be used to detect other marine or terrestrial regime shifts and distinguish between a linear and a nonlinear response to external forcing. For management purposes, distinguishing between these two types of forcing-response relationship producing regime shifts is critical, as they will lead to different management and policy incentives (Kelly

25 et al., 2015). For example, a routine monitoring of threshold-based systems leads to better management outcomes than "threshold-blind" management, i.e. when ignoring the possibility of a threshold and assuming a linear forcing-response relationship (Kelly et al., 2015).

The ability of OBGC models to simulate marine regime shifts suggests potential for predictability using coupled ocean–atmosphere general circulation models. For bottom-up marine regime shifts triggered by abrupt change in climatic forcing such as presented here, this may be achievable depending ultimately on the ability of coupled models to predict climate shifts. We showed that the observed SST shift in the late 1970s was well reproduced in the hindcast runs we analysed. Recent work suggests that the late 1970s climate shift is also produced realistically in the Coupled Model Intercomparison Project phase 5 multi-model hindcast simulations (Meehl and Teng, 2014). Therefore, climate shifts and their marine ecosystem response, such as the North Pacific 1970s regime shift studied here, may eventually be predictable using coupled models (or in simulations forced by the output of coupled models).

Appendix A

This appendix presents the results of the change point analysis for all parameters simulated from the five models. The physical parameters (SST and MLD) are omitted here as they are presented in Fig. 3. The chosen model for each variable and each OBGC model is presented in Table 3.

References

Alheit, J. P., Licandro, S., Coombs, A., Garcia, A., Giráldez, A., Garcia Santamaría, M. T., Slotte, A., and Tsikliras, A. C.: Atlantic Multidecadal Oscillation (AMO) modulates dynamics of small pelagic fishes and ecosystem regime shifts in the eastern North and Central Atlantic, J. Marine Syst., 131, 21–35, 2014.

Andersen, T., Carstensen, J., Hernandez-Garcia, E., and Duarte, D. M.: Ecological thresholds and regime shifts: approaches to identification, Trends Ecol. Evol., 24, 49–57, 2009.

Anderson, P. J. and Piatt, J. F.: Community reorganization of the Gulf of Alaska following ocean climate regime shift, Mar. Ecol.-Prog. Ser., 189, 117–123, 1999.

Baretta, J. W., Ebenhoh, W., and Ruardij, P.: The European Regional Seas Ecosystem Model, a complex marine ecosystem model, Neth. J. Sea Res., 33, 233–246, 1995.

Beaugrand, G.: The North Sea regime shift: evidence, causes, mechanisms and consequences, Prog. Oceanogr., 60, 245–262, 2004.

Beaugrand, G., Luczak, C., and Edwards, M.: Rapid biogeographical plankton shifts in the North Atlantic Ocean, Glob. Change Biol., 15, 1790–1803, 2009.

Beaulieu, C., Chen, J., and Sarmiento, J. L.: Change-point analysis as a tool to detect abrupt climate variations, Philos. T. R. Soc. A, 370, 1228–1249, 2012.

Beaulieu, C., Henson, S. A., Sarmiento, Jorge L., Dunne, J. P., Doney, S. C., Rykaczewski, R. R., and Bopp, L.: Factors challenging our ability to detect long-term trends in ocean chlorophyll, Biogeosciences, 10, 2711–2724, doi:10.5194/bg-10-2711-2013, 2013.

Bellwood, D. R., Hugues, T. P., Folke, C., and Nyström, M.: Confronting the coral reef crisis, Nature, 429, 827–833, 2004.

Benson, A. J. and Trites, A. W.: Ecological effects of regime shifts in the Bering Sea and eastern North Pacific Ocean, Fish Fish., 3, 95–113, 2002.

Bestelmeyer, B. T., Ellison, A. M., Fraser, W. R., Gorman, K. B., Holbrook, S. J., Laney, C. M., Ohman, M. D., Peters, D. P. C., Pillsbury, F. C., Rassweiler, A., Schmitt, R. J., and Sharma, S.: Analysis of abrupt transitions in ecological systems, Ecosphere, 2, 129, doi:10.1890/ES11-00216.1, 2011.

Blackford, J. C.: An analysis of benthic biological dynamics in a North Sea ecosystem model, J. Sea Res., 38, 213–230, 1997.

Blackford, J. C., Allen, J. I., and Gilbert, F. J.: Ecosystem dynamics at six contrasting sites: a generic modelling study, J. Marine Syst., 52, 191–215, 2004.

Marine regime shifts in ocean biogeochemical models

C. Beaulieu et al.

Brodeur, R. D. and Ware, D. M.: Long-term variability in zooplankton biomass in the subarctic Pacific Ocean, Fish. Oceanogr., 1, 32–38, 1992.

Buitenhuis, E., Hashioka, T., and Le Quéré, C.: Combined constraints on global ocean primary production using observations and models, Global Biogeochem. Cy., 27, 847–858, 2013.

5 Cury, P. and Shannon, L.: Regime shifts in upwelling ecosystems: observed changes and possible mechanisms in the northern and southern Benguela, Prog. Oceanogr., 60, 223–243, 2004.

Daskalov, G. M., Grishin, A. N., Rodionov, S., and Mihneva, V.: Trophic cascades triggered by overfishing reveal possible mechanisms of ecosystem regime shifts. P. Natl. Acad. Sci. USA,

10 104, 10518–10523, 2007.

de Young, B., Barange, M., Beaugrand, G., Harris, R., Perry, R. I., Scheffer, M., and Werner, F.: Regime shifts in marine ecosystems: detection, prediction and management, Trends Ecol. Evol., 23, 402–409, 2008.

Di Lorenzo, E. and Ohman, M. D.: A double-integration hypothesis to explain ocean ecosystem

15 response to climate forcing, P. Natl. Acad. Sci. USA, 110, 2496–2499, 2013.

Di Lorenzo, E., Schneider, N., Cobb, K. M., Franks, P. J. S., Chhak, K., Miller, A. J., McWilliams, J. C., Bograd, S. J., Arango, H., Curchitser, E., Powell, T. M., and Rivière, P.: North Pacific Gyre Oscillation links ocean climate and ecosystem change, Geophys. Res. Lett., 35, L08607, doi:10.1029/2007GL032838, 2008.

20 Drinkwater, K. F.: The regime shift of the 1920s and 1930s in the North Atlantic, Prog. Oceanogr., 68, 134–151, 2006.

Folke, C., Carpenter, S., Walker, B., Scheffer, M., Elmqvist, T., Gunderson, L., and Holling, C. S.: Regime shifts, resilience, and biodiversity in ecosystem management, Annu. Rev. Ecol. Evol. S., 35, 557–581, 2004.

25 Francis, R. C., Hare, S. R., Hollowed, A. B., and Wooster, W. S.: Effects of interdecadal climate variability on the oceanic ecosystems of the NE Pacific, Fish. Oceanogr., 7, 1–21, 1998.

Garcia, H. E., Locarnini, R. A., Boyer, T. P., Antonov, J. I., Baranova, O. K., Zweng, M. M., and Johnson, D. R.: World Ocean Atlas 2009, Volume 3: Dissolved Oxygen, Apparent Oxygen Utilization, and Oxygen Saturation, edited by: Levitus, S., NOAA Atlas NESDIS 70, US

30 Government Printing Office, Washington DC, 344 pp., 2009a.

Garcia, H. E., Locarnini, R. A., Boyer, T. P., Antonov, J. I., Baranova, O. K., Zweng, M. M., and Johnson, D. R.: World Ocean Atlas 2009, Volume 4: Nutrients (Phosphate, Nitrate, Silicate),

edited by: Levitus, S., NOAA Atlas NESDIS 71, US Government Printing Office, Washington DC, 398 pp., 2009b.

Halloran, P. R., Bell, T. G., and Totterdell, I. J.: Can we trust empirical marine DMS parameterisations within projections of future climate?, Biogeosciences, 7, 1645–1656, doi:10.5194/bg-7-1645-2010, 2010.

Hare, S. and Mantua, N. J.: Empirical evidence for North Pacific regime shifts in 1977 and 1989, Prog. Oceanogr., 47, 103–145, 2000.

Hasselmann, K.: Stochastic climate models. 1. Theory, Tellus, 28, 473–485, 1976.

Hsieh, C.-H., and Ohman, M. D.: Biological responses to environmental forcing: the linear tracking window hypothesis, Ecology, 87, 1932–1938, 2006.

Hunke, E. C. and Lipscomb, W. H.: CICE: The Los Alamos Sea Ice Model, Documentation and Software User's Manual, Version 4.0, Los Alamos National Laboratory Tech. Rep. LA-CC-06, Los Alamos, New Mexico, 2008.

Karnauskas, M., Schirripa, M. J., Craig, J. K., Cook, G. S., Kelble, C. R., Agar, J. J., Black, B. A., Enfield, D. A., Lindo-Atichatti, D., Muhling, B. A., Purcell, K. M., Richards, P. M., and Wang, C.: Evidence of climate-driven ecosystem reorganization in the Gulf of Mexico, Glob. Change Biol., 21, 2554–2568, 2015.

Kelly, R. P., Erickson, A. L., Mease, L. A., Battista, W., Kittinger, J. N., and Fujitta, R.: Embracing thresholds for better environmental management, Philos. T. R. Soc. B, 370, 20130276, doi:10.1098/rstb.2013.0276, 2015.

Key, R. M., Kozyr, A., Sabine, C. L., Lee, K., Wanningkhof, R., Bullister, J. L., Feely, R. A., Millero, F. J., Mordy, C., and Peng, T.-H.: A global ocean carbon climatology: results from Global Data Analysis Project (GLODAP), Global Biogeochem. Cy., 18, GB4031, doi:10.1029/2004GB002247, 2004.

Kwiatkowski, L., Yool, A., Allen, J. I., Anderson, T. R., Barciela, R., Buitenhuis, E. T., Butenschön, M., Enright, C., Halloran, P. R., Le Quéré, C., de Mora, L., Racault, M.-F., Sinha, B., Totterdell, I. J., and Cox, P. M.: iMarNet: an ocean biogeochemistry model intercomparison project within a common physical ocean modelling framework, Biogeosciences, 11, 7291–7304, doi:10.5194/bg-11-7291-2014, 2014.

Large, W. and Yeager, S.: The global climatology of an interannually varying air–sea flux data set, Clim. Dynam., 33, 341–364, 2009.

Le Quéré, C., Harrison, S. P., Prentice, I. C., Buitenhuis, E. T., Aumont, O., Bopp, L., Claustre, H., Da Cunha, L. C., Geider, R., Giraud, X., Klaas, C., Kohfeld, K. E., Legendre, L.,

Manizza, M., Platt, T., Rivkin, R. B., Sathyendranath, S., Uitz, J., Watson, A. J., and Wolf-Gladrow, D.: Ecosystem dynamics based on plankton functional types for global ocean bio-geochemistry models, Glob. Change Biol., 11, 2016–2040, 2005.

Lees, K., Pitois, S., Scott, C., Frid, C., and Mackinson, S.: Characterizing regime shifts in the marine environment, Fish Fish., 7, 104–127, 2006.

Lindegren, M., Blenckner, T., and Stenseth, N. C.: Nutrient reduction and climate change cause a potential shift from pelagic to benthic pathways in a eutrophic marine ecosystem, Glob. Change Biol., 18, 3491–3503, 2012.

Litzow, M. A. and Mueter, F. J.: Assessing the ecological importance of climate regime shifts: an approach from the North Pacific Ocean, Prog. Oceanogr., 120, 110–119, 2014.

Litzow, M. A., Mueter, F. J., and Hobday, A. J.: Reassessing regime shifts in the North Pacific: incremental climate change and commercial fishing are necessary for explaining decadal-scale biological variability, Glob. Change Biol., 20, 38–50, 2014.

Madec, G.: NEMO Reference Manual, Ocean Dynamic Component: NEMO-OPA, Note du Pôle de modélisation, Technical Report 27, Institut Pierre Simon Laplace, France, ISSN No. 1288–1619, 2008.

Mantua, N. J., Hare, S. R., Zhang, Y., Wallace, J. M., and Francis, R. C.: A Pacific interdecadal climate oscillation with impacts on salmon production, B. Am. Meteorol. Soc., 78, 1069–1079, 1997.

McGowan, J. A., Cayan, D. R., and Dorman, L. M.: Climate-ocean variability and ecosystem response in the Northeast Pacific, Science, 281, 210–217, 1998.

McQuatters-Gollop, A., Raitsos, D. E., Edwards, M., Pradhan, Y., Mee, L. D., Lavender, S. J., and Attrill, M. J.: A long-term chlorophyll data set reveals regime shift in North Sea phytoplankton biomass unconnected to nutrient trends, Limnol. Oceanogr., 52, 635–648, 2007.

Meehl, G. A. and Teng, H.: CMIP5 multi-model hindcasts for the mid-1970s shift and early 2000s hiatus and predictions for 2016–2035, Geophys. Res. Lett., 41, 1711–1716, 2014.

Möllmann, C., Diekmann, C., Müller-Karulis, B., Kornilovs, G., Plikshs, M., and Axe, P.: Reorganization of a large marine ecosystem due to atmospheric and anthropogenic pressure: a discontinuous regime shift in the Central Baltic Sea, Glob. Change Biol., 15, 1377–1393, 2009.

Overland, J., Rodionov, S., Minobe, S., and Bond, N.: North Pacific regime shifts: definitions, issues and recent transitions, Prog. Oceanogr., 77, 92–102, 2008.

Title Page

Abstract | Introduction

Conclusions | References

Tables | Figures

◄ | ►

◄ | ►

Back | Close

Full Screen / Esc

Printer-friendly Version

Interactive Discussion

Overland, J., Alheit, J., Bakun, A., Hurrell, J. H., Mackas, D. L., and Miller, A. J.: Climate controls on marine ecosystems and fish populations, J. Marine Syst., 79, 305–315, 2010.

Page, E. S.: Continuous inspection scheme, Biometrika, 41, 100–115, 1954.

Palmer, J. and Totterdell, I.: Production and export in a global ocean ecosystem model, Deep-Sea Res. Pt. I, 48, 1169–1198, 2001.

Paternoster, R., Brame, R., Mazerolle, P., and Piquero, A.: Using the correct statistical test for the equality of regression coefficients, Criminology, 36, 859–866, 1998.

Plagányi, É. E., Ellis, N., Blamey, L. K., Morello, E. B., Norman-Lopez, A., Robinson, W., Sporcic, M., and Sweatman, H.: Ecosystem modelling provides clues to understanding ecological tipping points, Mar. Ecol.-Prog. Ser., 512, 99–113, 2014.

Polovina, J. J., Mitchum, G. T., and Evans, G. T.: Decadal and basin-scale variation in mixed layer depth and the impact on biological production in the Central and North Pacific, 1960–88, Deep-Sea Res. Pt. I, 42, 1701–1716, 1995.

Reid, P. C., Borges, M. F., and Svendsen, E.: A regime shift in the North Sea circa 1988 linked to changes in the North Sea horse mackerel fishery, Fish. Res., 50, 163–171, 2001.

Rodionov, S. N.: A sequential algorithm for testing climate regime shifts, Geophys. Res. Lett., 31, L09204, doi:10.1029/2004GL019448, 2004.

Rudnick, D. L. and Davis, R. E.: Red noise and regime shifts, Deep-Sea Res. Pt. I, 50, 691–699, 2003.

Scheffer, M., Bascompte, J., Brock, W., Brovkin, V., Carpenter, S. R., Dakos, V., Held, H., van Nes, E. H., Rietkerk, M., and Sugihara, G.: Early-warning signals for critical transitions, Nature, 461, 53–59, 2009.

Schwing, F. B.: Regime shifts, physical forcing, in: Encyclopedia of Ocean Sciences (Second Edition), edited by: Steele, J. H., Academic Press, Oxford, 709–716, 2009.

Smith, T. M. and Reynolds, R. W.: Extended reconstruction of global sea surface temperatures based on COADS data (1854–1997), J. Climate, 16, 1495–1510, 2003.

Smith, T. M., Reynolds, R. W., Peterson, T. C., and Lawrimore, J.: Improvements to NOAA's Historical Merged Land–Ocean Surface Temperature Analysis (1880–2006), J. Climate, 21, 2283–2296, 2008.

Spencer, M., Birchenough, S. N. R., Mieszkowska, N., Robinson, L. A., Simpson, S. D., Burrows, M. T., Capasso, E., Cleall-Harding, P., Crummy, J., Duck, C., Eloire, D., Frost, M., Hall, A. J., Hawkins, S. J., Johns, D. G., Sims, T. D., Smyth, T. J., and Frid, C. L. J.: Temporal change in UK marine communities: trends or regime shifts?, Marine Ecol., 32, 10–24, 2011.

Marine regime shifts in ocean biogeochemical models

C. Beaulieu et al.

Title Page

Abstract	Introduction
Conclusions	References
Tables	Figures

Back | Close

Full Screen / Esc

Printer-friendly Version

Interactive Discussion

Van der Lingen, C., Shannon, L., Cury, P., Kreiner, A., Moloney, C., Roux, J., and Vaz-Velho, F.: Resource and ecosystem variability, including regime shifts, in the Benguela Current System, Lar. Mar. Ecosyst., 14, 147–184, 2006.

Yatsu, A., Aydin, K. Y., King, J. R., McFarlana, G. A., Chiba, S., Tadokoro, K., Kaeriyama, M., and Watanabe, Y.: Elucidating dynamic responses of North Pacific fish populations to climatic forcing: influence of life-history strategy, Prog. Oceanogr., 77, 252–268, 2008.

Yool, A., Popova, E. E., and Anderson, T. R.: Medusa-1.0: a new intermediate complexity plankton ecosystem model for the global domain, Geosci. Model Dev., 4, 381–417, doi:10.5194/gmd-4-381-2011, 2011.

Yool, A., Popova, E. E., and Anderson, T. R.: MEDUSA-2.0: an intermediate complexity biogeochemical model of the marine carbon cycle for climate change and ocean acidification studies, Geosci. Model Dev., 6, 1767–1811, doi:10.5194/gmd-6-1767-2013, 2013.

Title Page

Abstract | Introduction

Conclusions | References

Tables | Figures

|◄ | ►|

◄ | ►

Back | Close

Full Screen / Esc

Printer-friendly Version

Interactive Discussion

Table 1. Nutrient cycles and Plankton Functional Types represented in each model.

		HadOCC	Diat-HadOCC	MEDUSA	PlankTOM10	ERSEM
Nutrients	Nitrogen	×	×	×	×	×
	Phosphorous				×	×
	Silica		×	×	×	×
	Iron		×	×	×	×
	Carbon	×	×	×	×	×
	Alkalinity	×	×	×	×	×
Plankton Functional Type	Generic phytoplankton	×	×		×	
	Diatoms		×	×	×	×
	Large phytoplankton					×
	Picoplankton			×	×	×
	Coccolithophores				×	
	N_2 fixers				×	
	Flagellates					×
	Phaeocystis				×	
	Generic zooplankton	×	×			
	Microzooplankton			×	×	×
	Mesozooplankton			×	×	×
	Macrozooplankton				×	
	Heterotrophic nanoflagellates					×
	Bacteria				×	×
	Tracers	7	13	15	39	57

Table 2. List of models fitted in this study with their associated Schwarz Information Criterion (SIC) formulation.

Model description	Equations
(I) Constant mean	$y_t = \mu + \varepsilon_t$ $(t = 1, .., n)$ where y_t represents the time series, μ is the mean, ε_t are the random errors, t is the time and n is the length of the time series $\mathrm{SIC_I} = n \log(\mathrm{RSS}) + n(1 + \log(2\pi)) + (2 - n)\log(n)$ $\mathrm{RSS} = \sum_{i=1}^{n}(y_t - \hat{\mu})^2$, where $\hat{\mu}$ is the maximum likelihood estimates of μ
(II) Shift in the mean	$y_t = \begin{cases} \mu_1 + \varepsilon_t & (t = 1, .., p) \\ \mu_2 + \varepsilon_t & (t = p+1, .., n) \end{cases}$ where μ_1 and μ_2 are the means before and after the shift at time p $\mathrm{SIC_{II}} = n \log(\mathrm{RSS}) + n(1 + \log(2\pi)) + (3 - n)\log(n)$ $\mathrm{RSS} = \sum_{i=1}^{p}(y_t - \hat{\mu}_1)^2 + \sum_{i=p+1}^{n}(y_t - \hat{\mu}_2)^2$, where $\hat{\mu}_1$ and $\hat{\mu}_2$ are the maximum likelihood estimates of μ_1 and μ_2
(III) Linear trend	$y_t = \lambda + \beta t + \varepsilon_t$ $(t = 1, .., n)$ where λ is the intercept and β the trend of the linear regression model $\mathrm{SIC_{III}} = n \log(\mathrm{RSS}) + n(1 + \log(2\pi)) + (3 - n)\log(n)$ $\mathrm{RSS} = \sum_{i=1}^{n}\left(y_t - \hat{\lambda} - \hat{\beta}t\right)^2$, where $\hat{\lambda}$ and $\hat{\beta}$ are the maximum likelihood estimates of λ and β
(IV) Shift in the intercept and same linear trend	$y_t = \begin{cases} \lambda_1 + \beta t + \varepsilon_t & (t = 1, .., p) \\ \lambda_2 + \beta t + \varepsilon_t & (t = p+1, .., n) \end{cases}$ where λ_1 and λ_2 are the intercept before and after the shift $\mathrm{SIC_{IV}} = n \log(\mathrm{RSS}) + n(1 + \log(2\pi)) + (4 - n)\log(n)$ $\mathrm{RSS} = \sum_{i=1}^{p}\left(y_t - \hat{\lambda}_1 - \hat{\beta}t\right)^2 + \sum_{i=p+1}^{n}\left(y_t - \hat{\lambda}_2 - \hat{\beta}t\right)^2$, where $\hat{\lambda}_1$, $\hat{\lambda}_2$ and $\hat{\beta}$ are the maximum likelihood estimates of λ_1, λ_2 and β
(V) Shift in both the intercept and linear trend	$y_t = \begin{cases} \lambda_1 + \beta_1 t + \varepsilon_t & (t = 1, .., p) \\ \lambda_2 + \beta_2 t + \varepsilon_t & (t = p+1, .., n) \end{cases}$ where β_1 and β_2 are the trend before and after the shift $\mathrm{SIC_V} = n \log(\mathrm{RSS}) + n(1 + \log(2\pi)) + (5 - n)\log(n)$ $\mathrm{RSS} = \sum_{i=1}^{p}\left(y_t - \hat{\lambda}_1 - \hat{\beta}_1 t\right)^2 + \sum_{i=p+1}^{n}\left(y_t - \hat{\lambda}_2 - \hat{\beta}_2 t\right)^2$, where $\hat{\lambda}_1$, $\hat{\lambda}_2$, $\hat{\beta}_1$ and $\hat{\beta}_2$ are the maximum likelihood estimates of λ_1, λ_2, β_1 and β_2

All these models rely on the assumption that the random errors are independent and identically normally distributed ($\varepsilon_t \sim N(0, \sigma^2)$).

Table 3. Results from change point detection analysis for all observational and modelled time series.

	Parameter	Shift year	Shift type	SIC	SIC (Null model)	p value
Observations	SST	**1976**	trend and intercept	52.79	70.63	< 0.01[b]
All models	SST	**1976**	trend and intercept	58.39	74.15	< 0.01[b]
	MLD	1987	intercept	230.22	234.25	0.25
HadOCC	CHL	**1977**	mean	−138.40	−108.32	< 0.01[b]
	PP	**1991**	intercept	−264.06	−235.87	< 0.01[b,d]
	PHY	**1977**	mean	−211.46	−177.59	< 0.01[b]
	ZOO	**1977**	mean	−339.68	−315.70	< 0.01[b]
	DIN	**1977**	mean	139.52	175.85	< 0.01[b]
DiatHadOCC	CHL	**1976**	mean	−44.93	−13.82	< 0.01[b]
	PP	**1976**	mean	−216.45	−190.71	< 0.01[b]
	PHY	1976	intercept	−157.13	−155.59	0.53
	ZOO	1976	intercept	−298.90	−297.33	0.59
	DIN	**1978**	trend and intercept	151.10	202.7	< 0.01[b]
	SI	**1978**	trend and intercept	167.04	230.11	< 0.01[b]
	FE	**1978**	mean	−1035.5	−990.86	< 0.01[b]
MEDUSA	CHL	**1997**	intercept	−287.1	−274.71	0.01
	PP	**1991**	intercept	−308.90	−293.98	0.02
	PHY	**1961**	mean	−342.52	−328.88	< 0.01[b]
	ZOO	**1961**	mean	−260.89	−243.23	< 0.01[b]
	DIN	**1978**	trend and intercept	157.02	180.64	< 0.01[b]
	SI	1966	trend and intercept	201.11	217.83	0.09
	FE	1977	intercept	−946.48	−938.51	0.10
PlankTOM10	CHL	1978	intercept	−221.06	−214.48	0.24
	PP	**1991**	trend and intercept	−277.74	−258.29	< 0.01[b,d]
	PHY	1986	intercept	−1481.6	−1472.22	0.18
	ZOO	1988	intercept	−1427.8	−1414.98	0.16[c,d]
	DIN	1978	trend and intercept	48.07	62.65	0.07
	SI	1987	intercept	233.68	240.68	0.29
	FE	1983	intercept	−960.84	−954.91	0.12[c]
ERSEM	CHL	**1976**	mean	−162.70	−151.07	0.01[*]
	PP	1961	trend and intercept	−211.38	−207.73	0.49[d]
	PHY	**2002**	mean	95.40	101.6	0.04[a]
	ZOO	1961	trend and intercept	175.98	185.44	0.07
	DIN	1964	trend and intercept	6.58	16.48	0.10
	SI	**1991**	intercept	122.52	153.74	0.01[b]
	FE	1986	intercept	−414.51	−412.18	0.57

[a] p value < 0.05, [b] p value < 0.01, years in bold have a significant shift (p value < 0.05).
[c] Residuals not normally distributed (Lilliefors test, 5 % critical level).
[d] Residual variance not constant (Fisher test, 5 % critical level).

Table 4. Results from change point detection analysis on the first and second principal components of each model.

Model	PC	Shift year	Shift type	SIC	SIC (Null model)	p value
HadOCC	1	1987	intercept	230.44	234.39	0.26
	2	**1977**	mean	142.57	179.03	< 0.01[b]
DiatHadOCC	1	**1977**	intercept	225.30	250.17	0.05[a]
	2	1997	mean	230.77	235.39	0.17
MEDUSA	1	**1987**	trend and intercept	204.54	225.80	0.03[a]
	2	1987	intercept	235.47	235.87	0.59
PlankTOM10	1	1987	intercept	230.00	241.99	0.09
	2	1964	trend and intercept	231.01	233.01	0.41
ERSEM	1	**1987**	intercept	175.30	196.03	< 0.01[b]
	2	1993	intercept	213.52	219.11	0.20

[a] p value < 0.05, [b] p value < 0.01, years in bold have a significant shift (p value < 0.05).
[c] Residuals not normally distributed (Lilliefors test, 5 % critical level).
[d] Residual variance not constant (Fisher test, 5 % critical level).

Title Page

Abstract | Introduction

Conclusions | References

Tables | Figures

◄ | ►

◄ | ►

Back | Close

Full Screen / Esc

Printer-friendly Version

Interactive Discussion

Table 5. Results of the principal component analysis: percentage of variance explained by the first two components and relative contributions of the different variables to these two components. Variables with large relative contribution (> 10 %) to the two first components are in bold.

Model	PC	Variance explained (%)	Relative contribution (%)								
			SST	MLD	CHL	PP	PHY	ZOO	DIN	FE	SI
HadOCC	1	74.56	4.09	**94.48**	0.07	0.21	0.01	0.11	1.03	–	–
	2	23.68	**18.97**	0.01	4.12	0.55	2.00	0.46	**73.88**	–	–
DiatHadOCC	1	61.23	3.70	**13.91**	1.95	0.27	0.70	0.21	**36.71**	0.00	**42.55**
	2	35.37	1.46	**72.46**	0.32	0.23	0.04	0.10	**11.55**	0.00	**13.84**
MEDUSA	1	69.73	4.51	**15.04**	0.06	0.03	0.06	0.13	**15.85**	0.00	**64.32**
	2	25.96	0.13	**67.69**	0.20	0.12	0.08	0.20	**20.92**	0.00	**10.66**
PlankTOM10	1	75.43	3.41	**17.93**	0.76	0.65	0.00	0.00	**17.38**	0.00	**59.87**
	2	22.59	0.15	**72.75**	0.18	0.16	0.00	0.00	6.99	0.00	**19.77**
ERSEM	1	51.82	3.70	**26.45**	0.51	0.35	7.21	**28.17**	1.04	0.10	**32.48**
	2	34.27	1.13	**48.30**	0.42	0.61	2.84	**16.79**	5.79	0.05	**24.07**

Marine regime shifts in ocean biogeochemical models

C. Beaulieu et al.

Table 6. Forcing-response regressions in (1) HadOCC and Diat-HadOCC with SST as the physical forcing and in (2) MEDUSA and ERSEM with MLD as the physical forcing. The slopes of the linear regressions between the forcing and response before and after the shift are compared using a test of equality of two regression slopes.

| | | HadOCC | | | |
Forcing	Response	Slope 1957–1976 (standard error)	Slope 1977–2007 (standard error)	Test statistic	p value
SST	CHL	−0.025 (0.028)	−0.008 (0.024)	1.407	0.166
	PP	0.000 (0.005)	0.021 (0.011)	−1.703	0.095
	TPHY	−0.008 (0.014)	−0.030 (0.013)	1.179	0.245
	TZOO	0.002 (0.004)	−0.012 (0.003)	2.823	0.007[a]
		Diat-HadOCC			
SST	CHL	−0.121 (0.071)	−0.217 (0.052)	1.095	0.279
	PP	−0.033 (0.012)[c]	−0.022 (0.012)	−0.666	0.508
	TPHY	−0.028 (0.025)	−0.069 (0.018)	1.345	0.185
	TZOO	−0.002 (0.006)	−0.018 (0.005)	2.034	0.048[a]
		MEDUSA			
Forcing	Response	Slope 1957–1988 (standard error)	Slope 1989–2007 (standard error)	Test statistic	p value
MLD	CHL	0.001 (0.001)	0.003 (0.002)	−1.045	0.302
	PP	0.001 (0.001)	0.002 (0.002)[c]	−0.553	0.583
	TPHY	−0.002 (0.001)	−0.001 (0.001)	−1.056	0.296
	TZOO	−0.004 (0.002)	−0.003 (0.002)[c]	−0.740	0.464
		ERSEM			
MLD	CHL	−0.006 (0.005)[b]	0.003 (0.005)	1.315	0.195
	PP	0.001 (0.003)	0.006 (0.003)	1.076	0.288
	TPHY	−0.060 (0.053)	−0.044 (0.071)	0.184	0.854
	TZOO	−0.231 (0.160)	−0.047 (0.143)	0.859	0.395

[a] p value < 0.05.
[b] Residuals not normally distributed (Lilliefors test, 5 % critical level).
[c] Residual variance not constant (Breusch Pagan test, 5 % critical level).
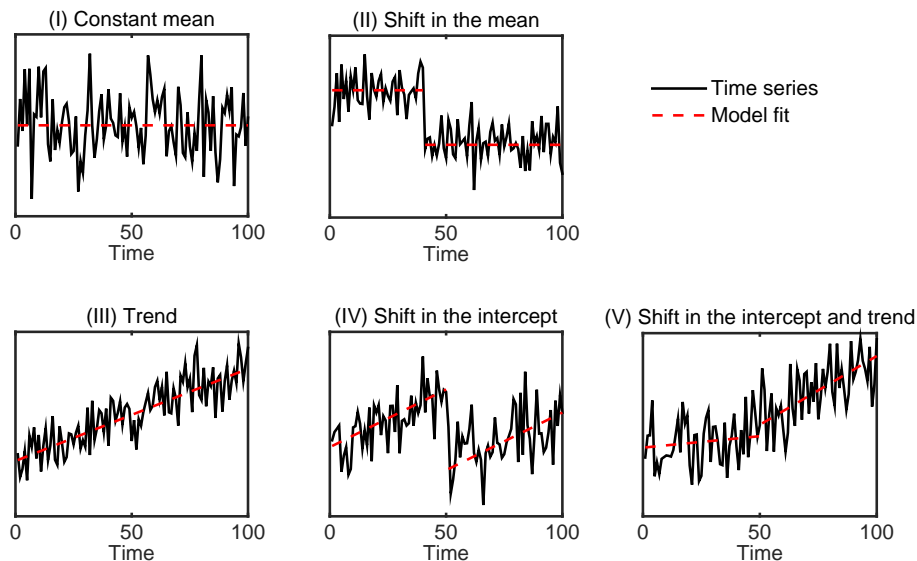
Figure 1. Five types of statistical models that were fitted to the data. The solid lines are synthetic time series drawn from a model with (I) a constant mean, (II) shift in the mean, (III) trend, (IV) shift in the intercept of the trend (the trend is the same before and after the shift) and (V) shift in both the intercept and trend. The constant mean (I) is the null model for a shift in the mean (II) when testing for significance. Similarly, the trend model (III) is the null model to test the shift significance when the model selected is either a shift in the intercept (IV) or a shift in both the intercept and trend (V). The corresponding models are further described in Table 2. Figure adapted from Beaulieu et al. (2012).
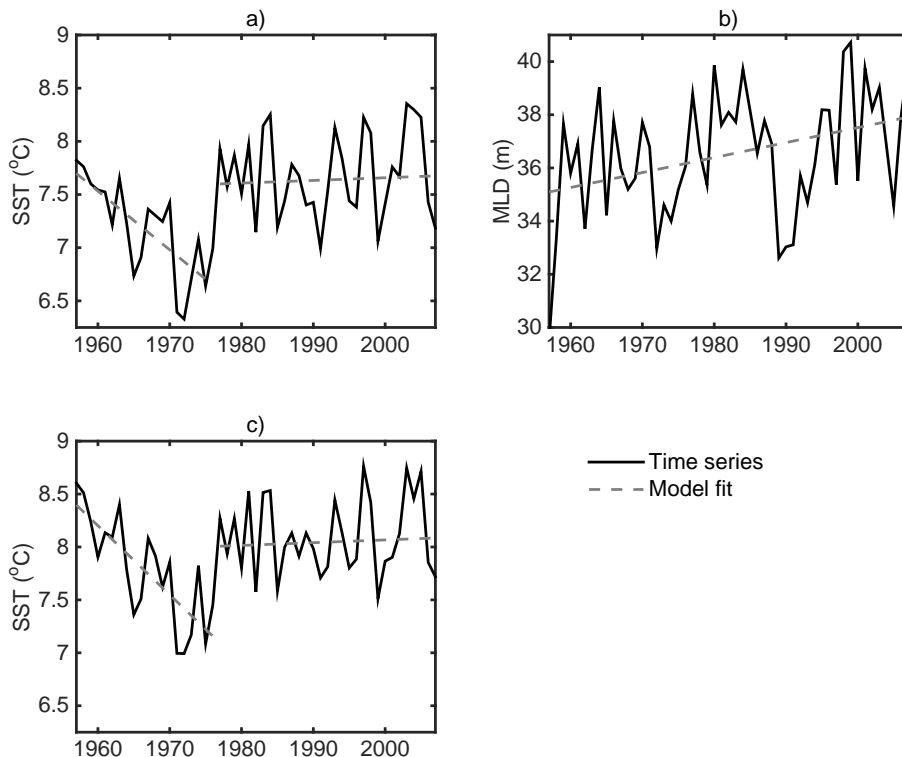
Figure 2. Simulated time series of mean SST **(a)** and MLD **(b)** for the Gulf of Alaska. These time series are the same in all 5 OBGC models used. **(c)** Observed time series of mean SST for the Gulf of Alaska. The red dotted lines represent the statistical model chosen (see Table 3) to fit these time series. Both the simulated SST and observed SST are best fit with a statistical model exhibiting a shift in intercept and trend occurring in 1976 (significant at the 5 % critical level, see Table 3). The MLD time series does not exhibit a significant shift and is best represented by a linear trend.
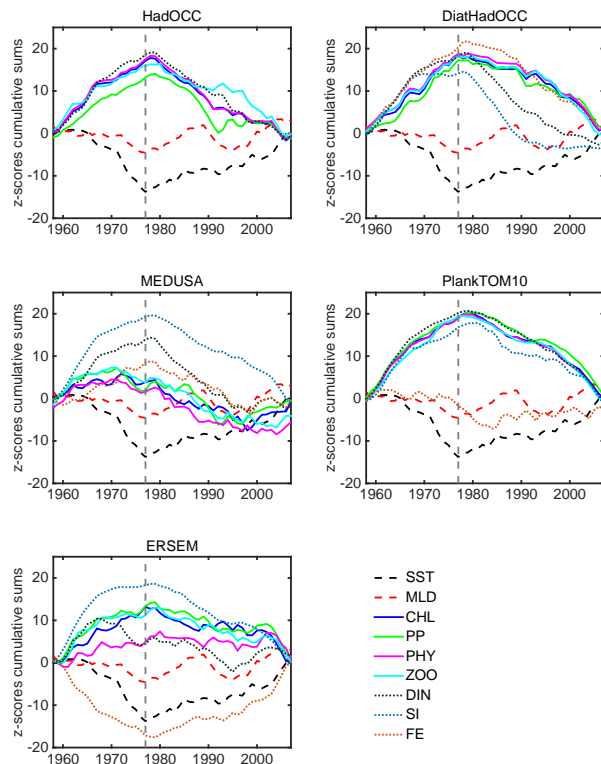
Figure 3. Cumulative sums of the *z* scores of sea surface temperature (SST), mixed layer depth (MLD), surface dissolved inorganic nitrogen (DIN), silica (SI), iron (FE), surface chlorophyll (CHL), integrated primary production (PP), total surface phytoplankton (PHY) and zooplankton (ZOO) biomass for each model averaged over the Gulf of Alaska region. *Z* scores are calculated by subtracting the mean and dividing by the standard deviation of each time series. Cumulative sums of the *z* scores are then calculated. The vertical lines in 1977 provide a guide to the eye showing where the slopes change after 1977.
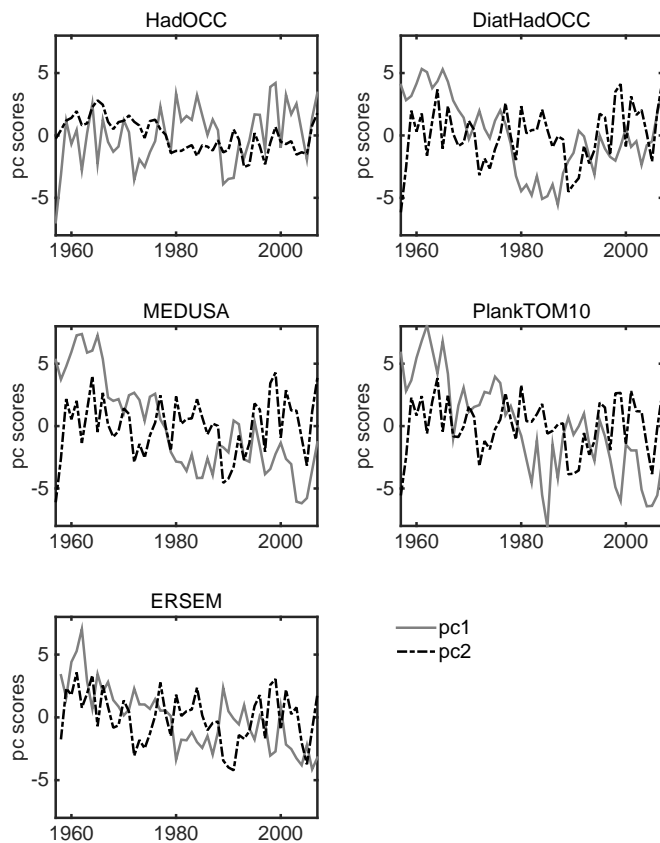
Figure 4. First and second principal components of sea surface temperature, mixed layer depth, surface dissolved inorganic nitrogen, silica, iron, surface chlorophyll, integrated primary production, total surface phytoplankton and zooplankton biomass (if available) for each model averaged over the Gulf of Alaska region.

Title Page

Abstract | Introduction

Conclusions | References

Tables | Figures

|◄ | ►|

◄ | ►

Back | Close

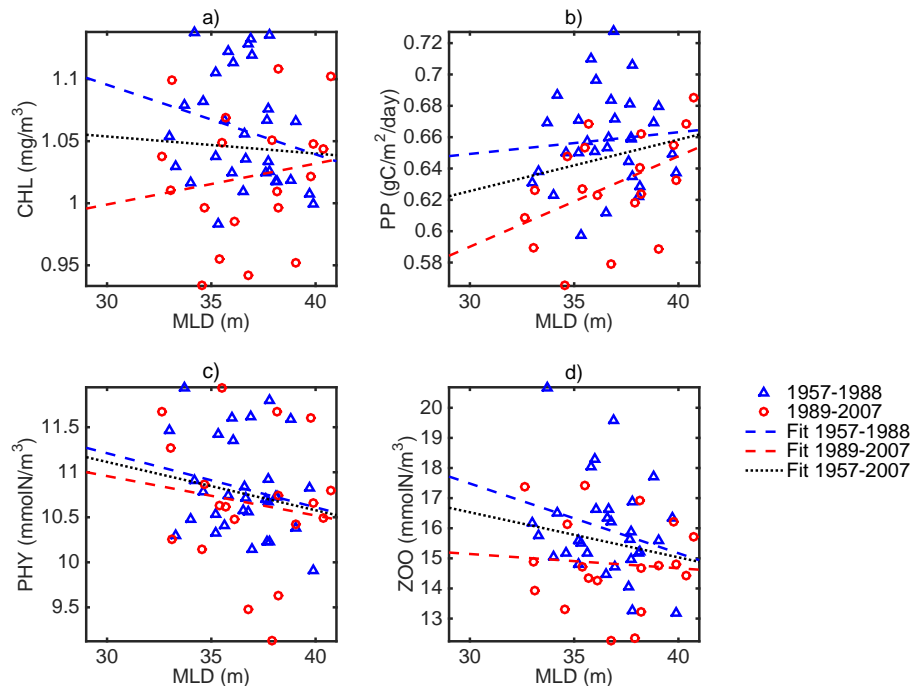Full Screen / Esc

Printer-friendly Version

Interactive Discussion
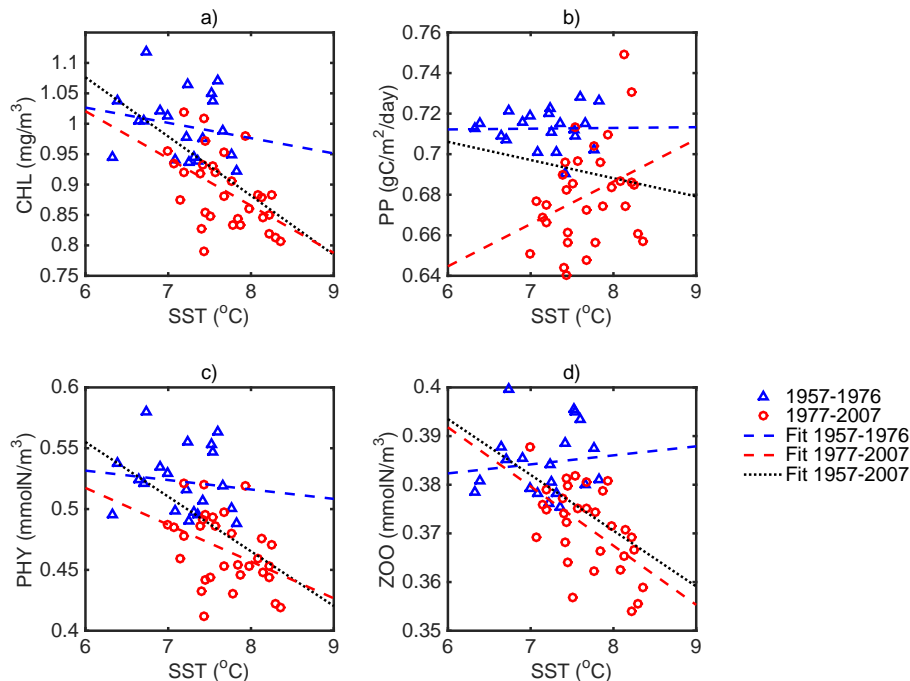
Figure 5. Relationships between sea surface temperature (SST) and **(a)** surface chlorophyll (CHL), **(b)** integrated primary production (PP), **(c)** total surface phytoplankton (PHY) and **(d)** zooplankton biomass (ZOO) for HadOCC over the Gulf of Alaska region. Linear relationships are inferred for the periods 1957–1976, 1977–2007 and 1957–2007 using least square regression.

Figure 6. Relationships between sea surface temperature (SST) and **(a)** surface chlorophyll (CHL), **(b)** integrated primary production (PP), **(c)** total surface phytoplankton (PHY) and **(d)** zooplankton biomass (ZOO) for Diat-HadOCC over the Gulf of Alaska region. Linear relationships are inferred for the periods 1957–1976, 1977–2007 and 1957–2007 using least square regression.

Title Page

Abstract | Introduction

Conclusions | References

Tables | Figures

|◄ | ►|

◄ | ►

Back | Close

Full Screen / Esc

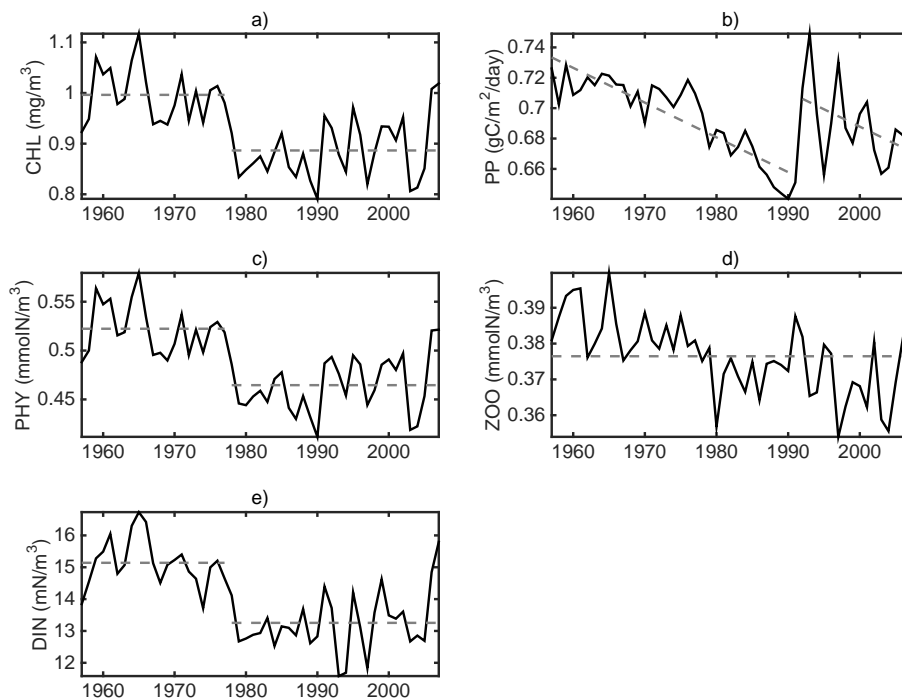Printer-friendly Version

Interactive Discussion
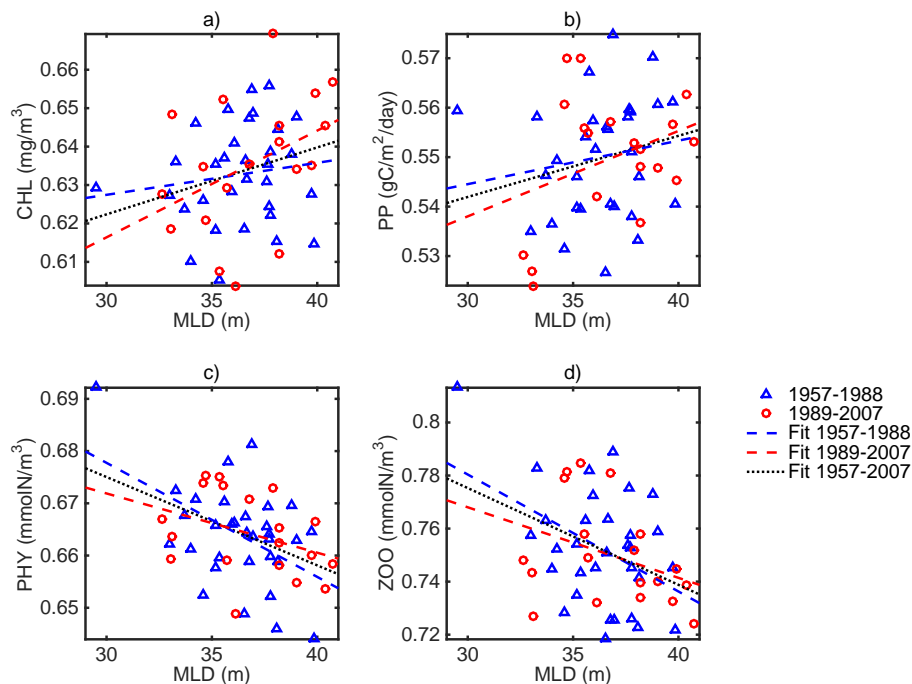
Figure 7. Relationships between mixed layer depth (MLD) and **(a)** surface chlorophyll (CHL), **(b)** integrated primary production (PP), **(c)** total surface phytoplankton (PHY) and **(d)** zooplankton (ZOO) biomass for MEDUSA over the Gulf of Alaska region. Linear relationships are inferred for the periods 1957–1988, 1989–2007 and 1957–2007 using least square regression.

Figure 8. Relationships between mixed layer depth (MLD) and **(a)** surface chlorophyll (CHL), **(b)** integrated primary production (PP), **(c)** total surface phytoplankton (PHY) and **(d)** zooplankton (ZOO) biomass for ERSEM over the Gulf of Alaska region. Linear relationships are inferred for the periods 1957–1988, 1989–2007 and 1957–2007 using least square regression.

Figure A1. Time series of **(a)** surface chlorophyll, **(b)** integrated primary production, **(c)** total surface phytoplankton, **(d)** zooplankton biomass and **(e)** surface dissolved inorganic nitrogen simulated with the HadOCC model and averaged over the Gulf of Alaska region. The dotted lines represent the statistical model selected.
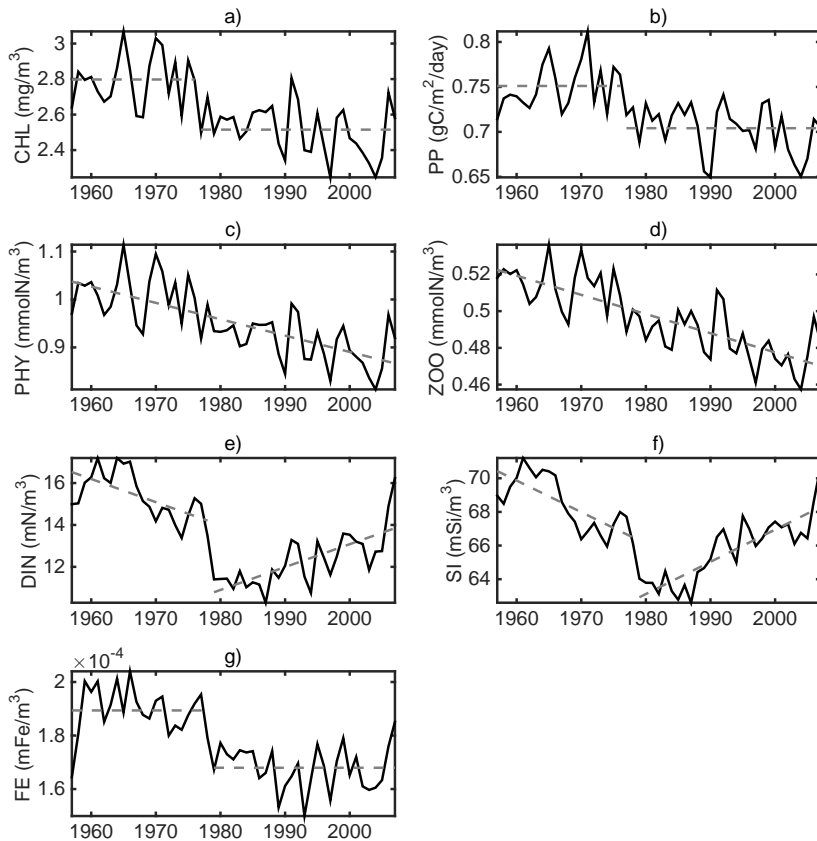
Figure A2. Time series of **(a)** surface chlorophyll, **(b)** integrated primary production, **(c)** total surface phytoplankton, **(d)** zooplankton biomass and **(e)** surface dissolved inorganic nitrogen, **(f)** silica and **(g)** iron simulated with the DiatHadOCC model and averaged over the Gulf of Alaska region. The dotted lines represent the statistical model selected.

Figure A3. Time series of **(a)** surface chlorophyll, **(b)** integrated primary production, **(c)** total surface phytoplankton, **(d)** zooplankton biomass and **(e)** surface dissolved inorganic nitrogen, **(f)** silica and **(g)** iron simulated with the MEDUSA model and averaged over the Gulf of Alaska region. The dotted lines represent the statistical model selected.

Title Page

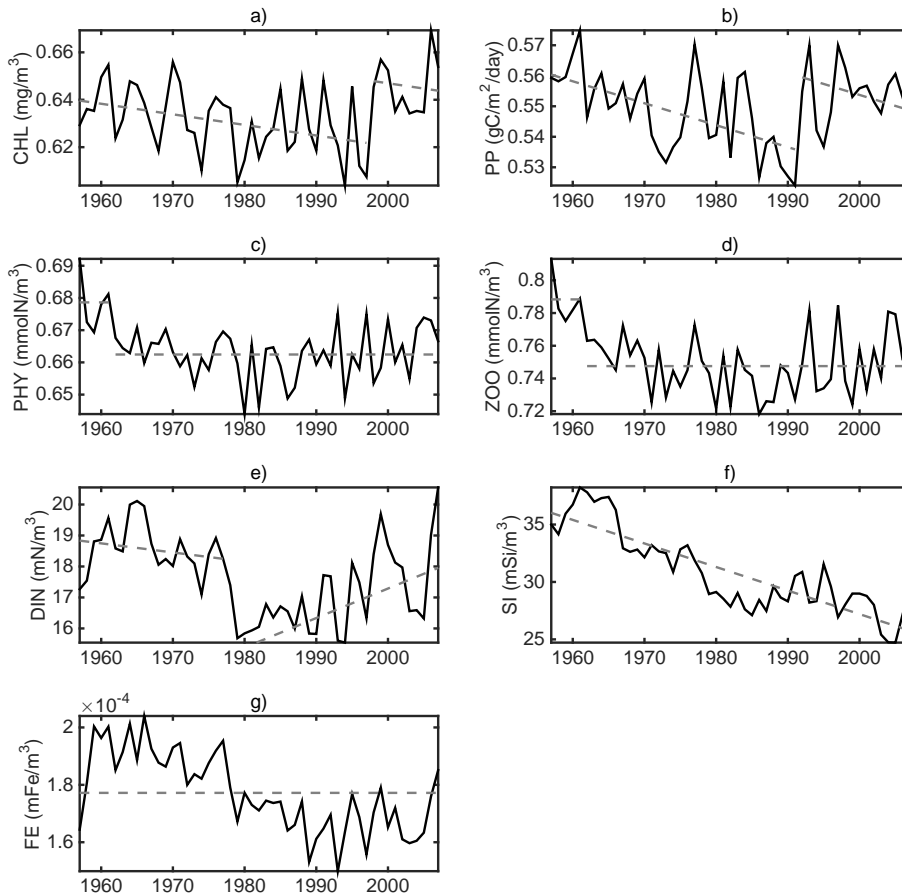Abstract · Introduction

Conclusions · References

Tables · Figures

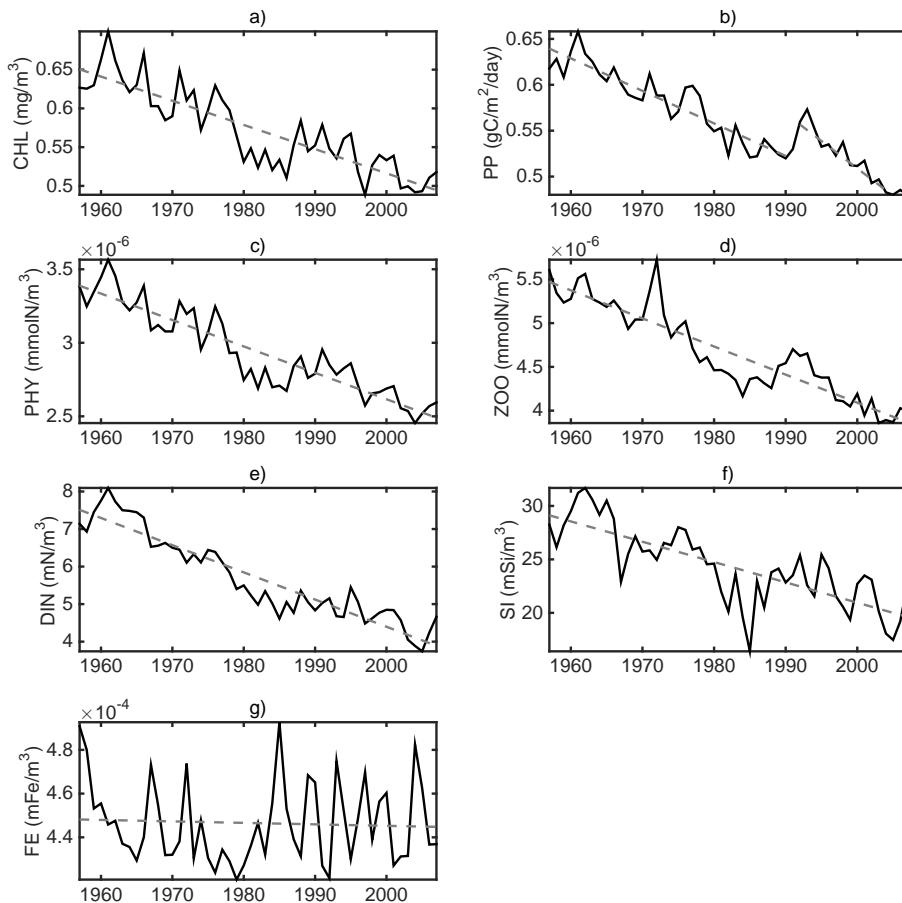|◄ · ►|

◄ · ►

Back · Close

Full Screen / Esc

Printer-friendly Version

Interactive Discussion

Figure A4. Time series of **(a)** surface chlorophyll, **(b)** integrated primary production, **(c)** total surface phytoplankton, **(d)** zooplankton biomass and **(e)** surface dissolved inorganic nitrogen, **(f)** silica and **(g)** iron simulated with the PlankTOM10 model and averaged over the Gulf of Alaska region. The dotted lines represent the statistical model selected.

Title Page

Abstract | Introduction

Conclusions | References
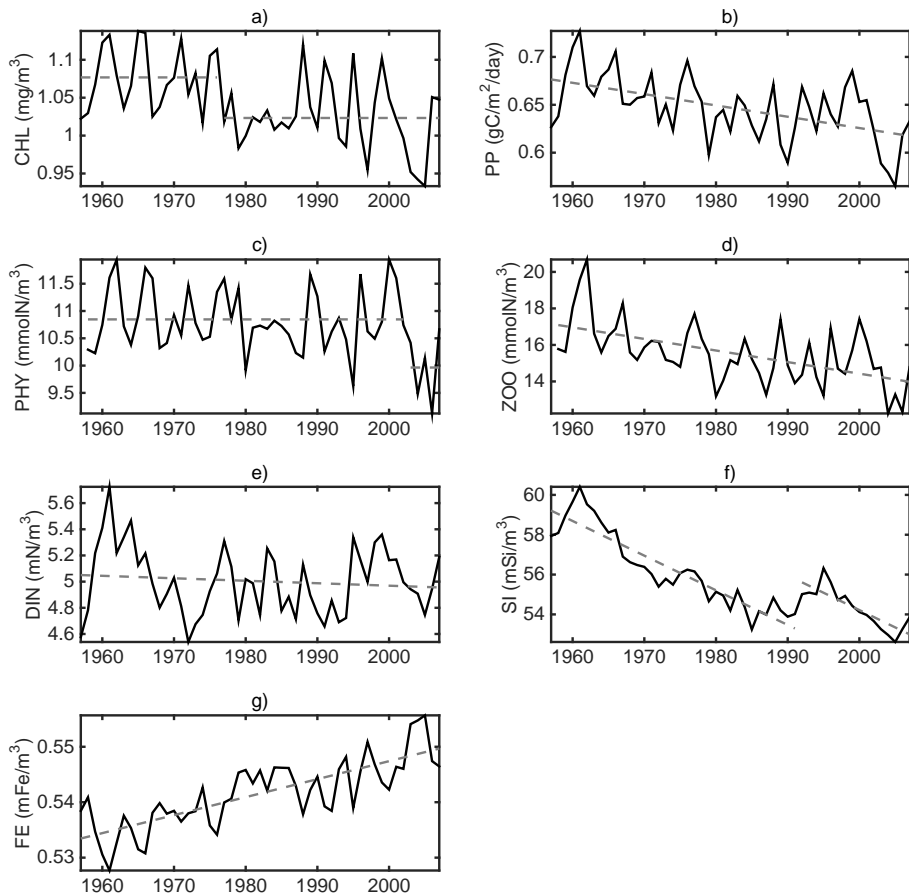
Tables | Figures

|◄ | ►|

◄ | ►

Back | Close

Full Screen / Esc

Printer-friendly Version

Interactive Discussion

Figure A5. Time series of **(a)** surface chlorophyll, **(b)** integrated primary production, **(c)** total surface phytoplankton, **(d)** zooplankton biomass and **(e)** surface dissolved inorganic nitrogen, **(f)** silica and **(g)** iron simulated with the ERSEM model and averaged over the Gulf of Alaska region. The dotted lines represent the statistical model selected.

Title Page

Abstract | Introduction

Conclusions | References

Tables | Figures

|◄ | ►|

◄ | ►

Back | Close

Full Screen / Esc

Printer-friendly Version

Interactive Discussion